

MATHEMATICAL MODELING OF GAS COMBUSTION IN A TWISTED JET AND OF THE FORMATION OF A FIERY WHIRLWIND

A. M. Grishin, O. V. Matvienko,
and Yu. A. Rudi

UDC 533.656:662.969

Numerical simulation of fiery whirlwinds originating as a result of blowing-in of a twisted flow of a fuel gas into an initially stagnant medium is carried out. The results of calculations agree with experimental values in the entire range of twistings studied.

Keywords: whirlwind, convective column, twisted flows, turbulence, heat exchange, combustion, chemical reaction, mathematical modeling.

Introduction. It is known [1–3] that a convective column of an ascending gas appears over the area of a forest fire. In the presence of circulation of the surrounding medium, the vorticity intrudes into the convective column, thus preventing turbulent diffusion and air influx into the flow core. As a result, a long narrow column of a rotating gas called a fiery whirlwind occurs. In [4, 5], some of the laws governing the formation of thermal and fiery whirlwinds were obtained experimentally.

In [6], a complex investigation of free convective flows is carried out. In [7], a review and classification of different types of vortices, including fiery whirlwinds, are given. In [8], an analysis of an experimental investigation of a turbulent jet burning inside a twisted flow organized by rotation of a cylindrical wire screen is carried out. The results of the computational-experimental investigation of the combustion of a twisted jet of kerosene vapors performed in [9] show that for the formation of fiery whirlwinds the presence of external vorticity and of a vertical flow acceleration is needed. In [10, 11], a mathematical model of the formation of a convective column and of a fiery whirlwind in forest fires is formulated and some of the results of mathematical modeling are given.

The aim of the present work is to improve the physical model suggested in [4, 5] and mathematically model the fiery whirlwinds appearing as a result of blowing-in of a twisted fuel gas flow (carbon monoxide) into an initially stagnant medium (air).

Mathematical Model of a Fiery Whirlwind. For the mathematical statement of the problem we assume that:

- 1) the flow in the region considered is axisymmetric;
- 2) the gas flow is twisted at the entrance according to the law of solid body rotation;
- 3) the air motion is characterized by the presence of regions of laminar, transient, and of turbulent modes of flow;
- 4) combustion proceeds in a diffusion-kinetic regime, i.e., the rate of combustion is determined by both the chemical kinetics and the processes of turbulent mixing.

To calculate the characteristics of motion and heat transfer, we use the Reynolds equations [12]. The turbulence characteristics were calculated on the basis of a two-parameter model with the use of equations for the kinetic energy of turbulence k and for the rate of its dissipation ϵ with allowance for the action of buoyancy forces, smallness of Reynolds numbers [13], as well as for the anisotropy of turbulent pulsations [14], and for the influence of twisting on the turbulent flow stability [15]. The temperature dependence of the molecular dynamic viscosity was calculated with the aid of the Sutherland equation [16, 17]. The viscosity of a mixture of gases was determined using Wilke's equation [10].

To describe the process of combustion, apart from the energy equation we used the conservation equations for the mass of the components O_2 , CO , CO_2 , and N_2 with allowance for the progress of an irreversible exothermal chemical reaction in the flow: $2CO + O_2 \rightarrow 2CO_2 + Q$. Combustion in turbulent diffusion flames is determined by both

Tomsk State University, 36 Lenin Ave., Tomsk, 634050, Russia; email: matvoleg@mail.ru. Translated from Inzhenerno-Fizicheskii Zhurnal, Vol. 82, No. 5, pp. 902–908, September–October, 2009. Original article submitted May 28, 2008.

the chemical kinetics and the processes of turbulent mixing. Within the framework of the kinetic model, the rate of a chemical reaction is described by the Arrhenius law, which is valid for a laminar mode of flow of a mixture of a fuel and an oxidant.

The eddy dissipation model has been developed for describing turbulent diffusion flames and based on the assumption that chemical reactions very rapidly bring a reacting mixture to an equilibrium state. Thus, the rate of a chemical reaction for diffusion flames is determined by the rate of turbulent mixing of a combustible and an oxidant. According to this model, to initiate the process of combustion it is sufficient that a combustible and an oxidant (usually air) be in the same control volume.

As the criterion that characterizes the mode of combustion we may use the turbulent Damköhler number [18]:

$$Da = K\rho \exp\left(-\frac{E}{RT}\right) \frac{k}{\varepsilon}. \quad (1)$$

If $Da \leq 1$, the chemical reaction is determined by the Arrhenius kinetics, or otherwise by the processes of turbulent mixing [18]. Thus, the rate of a chemical reaction Φ can be represented in the form [18]

$$\Phi = \begin{cases} K\rho^2 M_{ox} M_{fl} \exp\left(-\frac{E}{RT}\right), & Da \leq 1; \\ B\rho^2 \min[M_{ox}, 2M_{fl}] \frac{\varepsilon}{k}, & 1 < Da. \end{cases} \quad (2)$$

With allowance for the foregoing, we have a system of equations

$$\frac{\partial \rho v_z}{\partial z} + \frac{1}{r} \frac{\partial \rho v_r r}{\partial r} = 0, \quad (3)$$

$$\frac{\partial \rho v_z^2}{\partial z} + \frac{1}{r} \frac{\partial \rho v_z v_r r}{\partial r} = -\frac{\partial p}{\partial z} + \frac{\partial}{\partial z} \left[\mu_{zz} \left(2 \frac{\partial v_z}{\partial z} - \frac{2}{3} \left(\frac{\partial v_z}{\partial z} + \frac{1}{r} \frac{\partial v_r r}{\partial r} \right) \right) \right] + \frac{1}{r} \frac{\partial}{\partial r} \left[\mu_{zr} r \left(\frac{\partial v_z}{\partial r} + \frac{\partial v_r}{\partial z} \right) \right] - (\rho - \rho_e) g, \quad (4)$$

$$\begin{aligned} \frac{\partial \rho v_z v_r}{\partial z} + \frac{1}{r} \frac{\partial \rho v_r^2 r}{\partial r} &= -\frac{\partial p}{\partial r} + \frac{\partial}{\partial z} \left[\mu_{zr} \left(\frac{\partial v_r}{\partial z} + \frac{\partial v_z}{\partial r} \right) \right] \\ &+ \frac{1}{r} \frac{\partial}{\partial r} \left[\mu_{rr} r \left(2 \frac{\partial v_r}{\partial r} - \frac{2}{3} \left(\frac{\partial v_z}{\partial z} + \frac{1}{r} \frac{\partial v_r r}{\partial r} \right) \right) \right] - \mu_{rr} \frac{v_r}{r} + \frac{\rho v_\phi^2}{r}, \end{aligned} \quad (5)$$

$$\frac{\partial \rho v_z v_\phi}{\partial z} + \frac{1}{r} \frac{\partial \rho v_r v_\phi r}{\partial r} = \frac{\partial}{\partial z} \left[\mu_{z\phi} \frac{\partial v_z}{\partial z} \right] + \frac{1}{r^2} \frac{\partial}{\partial r} \left[\mu_{r\phi} r^3 \frac{\partial}{\partial r} \left(\frac{v_z}{r} \right) \right] - \frac{\rho v_r v_\phi}{r}, \quad (6)$$

$$\frac{\partial \rho v_z k}{\partial z} + \frac{1}{r} \frac{\partial \rho v_r kr}{\partial r} = \frac{\partial}{\partial z} \left[\frac{\mu_{eff}}{\sigma_k} \frac{\partial k}{\partial z} \right] + \frac{1}{r} \frac{\partial}{\partial r} \left[\frac{\mu_{eff}}{\sigma_k} r \frac{\partial k}{\partial r} \right] + G_k + P - I - \rho \varepsilon, \quad (7)$$

$$\frac{\partial \rho v_z \varepsilon}{\partial z} + \frac{1}{r} \frac{\partial \rho v_r \varepsilon r}{\partial r} = \frac{\partial}{\partial z} \left[\frac{\mu_{eff}}{\sigma_\varepsilon} \frac{\partial \varepsilon}{\partial z} \right] + \frac{1}{r} \frac{\partial}{\partial r} \left[\frac{\mu_{eff}}{\sigma_\varepsilon} r \frac{\partial \varepsilon}{\partial r} \right]$$

$$+ C_{1\epsilon} \left(G_k + C_{3\epsilon} \max(0, P) + C'_{1\epsilon} v_\phi \frac{\partial}{\partial r} \left(\frac{v_\phi}{r} \right) \right) \frac{\epsilon}{k} - C_{2\epsilon} f_{2\epsilon} \rho \epsilon \left(1 - C'_{2\epsilon} \frac{k^2}{\epsilon^2} \frac{v_\phi}{r^2} \frac{\partial v_\phi}{\partial r} \right) \frac{\epsilon}{k}, \quad (8)$$

$$c_p \left(\frac{\partial \rho v_z T}{\partial z} + \frac{1}{r} \frac{\partial \rho v_r r T}{\partial r} \right) = \frac{\partial}{\partial z} \left[\lambda_{\text{eff}} \frac{\partial T}{\partial z} \right] + \frac{1}{r} \frac{\partial}{\partial r} \left[\lambda_{\text{eff}} r \frac{\partial T}{\partial r} \right] + Q \Phi, \quad (9)$$

$$\frac{\partial \rho v_z M_{\text{fl}}}{\partial z} + \frac{1}{r} \frac{\partial \rho v_r r M_{\text{fl}}}{\partial r} = \frac{\partial}{\partial z} \left[\rho D_{\text{eff}} \frac{\partial M_{\text{fl}}}{\partial z} \right] + \frac{1}{r} \frac{\partial}{\partial r} \left[\rho D_{\text{eff}} r \frac{\partial M_{\text{fl}}}{\partial r} \right] - 2 \frac{W_{\text{fl}}}{W_{\text{ox}}} \Phi, \quad (10)$$

$$\frac{\partial \rho v_z M_{\text{ox}}}{\partial z} + \frac{1}{r} \frac{\partial \rho v_r r M_{\text{ox}}}{\partial r} = \frac{\partial}{\partial z} \left[\rho D_{\text{eff}} \frac{\partial M_{\text{ox}}}{\partial z} \right] + \frac{1}{r} \frac{\partial}{\partial r} \left[\rho D_{\text{eff}} r \frac{\partial M_{\text{ox}}}{\partial r} \right] - \Phi, \quad (11)$$

$$\frac{\partial \rho v_z M_{\text{pr}}}{\partial z} + \frac{1}{r} \frac{\partial \rho v_r r M_{\text{pr}}}{\partial r} = \frac{\partial}{\partial z} \left[\rho D_{\text{eff}} \frac{\partial M_{\text{pr}}}{\partial z} \right] + \frac{1}{r} \frac{\partial}{\partial r} \left[\rho D_{\text{eff}} r \frac{\partial M_{\text{pr}}}{\partial r} \right] + 2 \frac{W_{\text{pr}}}{W_{\text{ox}}} \Phi, \quad (12)$$

$$\frac{\partial \rho v_z M_{\text{in}}}{\partial z} + \frac{1}{r} \frac{\partial \rho v_r r M_{\text{in}}}{\partial r} = \frac{\partial}{\partial z} \left[\rho D_{\text{eff}} \frac{\partial M_{\text{in}}}{\partial z} \right] + \frac{1}{r} \frac{\partial}{\partial r} \left[\rho D_{\text{eff}} r \frac{\partial M_{\text{in}}}{\partial r} \right], \quad (13)$$

$$\rho = \frac{p}{RT} \left(\frac{M_{\text{fl}}}{W_{\text{fl}}} + \frac{M_{\text{ox}}}{W_{\text{ox}}} + \frac{M_{\text{pr}}}{W_{\text{pr}}} + \frac{M_{\text{in}}}{W_{\text{in}}} \right)^{-1}. \quad (14)$$

The parameters and functions entering into Eqs. (3)–(14) were calculated using the relations

$$\begin{aligned} \mu_{ij} &= \mu_0 + C_\mu f_\mu \alpha_{ij} \rho \frac{k^2}{\epsilon}, \quad ij = zz, zr, z\phi, rr, r\phi, \phi\phi; \quad \alpha_{ij} = \begin{pmatrix} 1.04 & 0.01 & 1 \\ 0.01 & 0.1 & 0.025 \\ 1 & 0.025 & 1 \end{pmatrix}, \\ \mu_t &= C_\mu f_\mu \rho \frac{k^2}{\epsilon}, \quad \mu_{\text{eff}} = \mu_0 + \mu_t, \\ G_k &= \mu_t \left\{ 2 \left[\left(\frac{\partial v_z}{\partial z} \right)^2 + \left(\frac{\partial v_r}{\partial r} \right)^2 + \left(\frac{v_r}{r} \right)^2 \right] + \left(\frac{\partial v_z}{\partial r} \right)^2 + \left(\frac{\partial v_r}{\partial z} \right)^2 + \left(r \frac{\partial}{\partial r} \left(\frac{v_\phi}{r} \right) \right)^2 \right\}, \\ P &= - \frac{\mu_t g}{\rho \sigma_k} \frac{\partial \rho}{\partial z}, \quad I = 2 \mu_t (\text{grad } \sqrt{k})^2, \\ J &= 2 \frac{\mu_0 \mu_t}{\rho} \left[\left(\frac{1}{r} \frac{\partial}{\partial r} \left(r \frac{\partial v_z}{\partial r} \right) + \frac{\partial^2 v_z}{\partial z^2} \right)^2 + \left(\frac{1}{r} \frac{\partial}{\partial r} \left(r \frac{\partial v_r}{\partial r} \right) - \frac{v_r}{r^2} + \frac{\partial^2 v_r}{\partial z^2} \right)^2 + \left(\frac{1}{r} \frac{\partial}{\partial r} \left(r \frac{\partial v_\phi}{\partial r} \right) - \frac{v_\phi}{r^2} + \frac{\partial^2 v_\phi}{\partial z^2} \right)^2 \right], \\ f_\mu &= \exp \left[- \frac{3.4}{(1 + 0.02 \text{Re}_t)^2} \right], \quad f_2 = 1 - 0.3 \exp(-\text{Re}_t^2), \quad \text{Re}_t = \frac{\rho k^2}{\mu_0 \epsilon}, \end{aligned}$$

TABLE 1. The Sutherland Coefficient γ and Values of Dynamic Viscosity μ_0 at the Temperature $T_* = 300$ K

Gas	γ, K	$\mu_0 \cdot 10^6, \text{Pa}\cdot\text{sec}$
Oxygen	138	20.63
Carbon monoxide	102	17.84
Carbon dioxide	255	14.96
Nitrogen	107	17.84

$$\begin{aligned} \mu_{0,i} &= \mu_{*,i} \frac{\gamma_i + T_{*,k}}{\gamma_i + T} \left(\frac{T}{T_{*,i}} \right)^{3/2}, \quad i = \text{fl, ox, pr, in}; \\ \mu_0 &= \sum_{i=1}^4 \frac{\mu_{0,i} \xi_k}{\sum_{j=1}^4 \xi_j \Psi_{ij}}, \quad \xi_i = \frac{M_i/W_i}{\sum_{j=1}^4 M_j/W_j}, \quad \Psi_{ij} = \frac{1}{2\sqrt{2}} \left(1 + \frac{W_i}{W_j} \right)^{-1/2} \left[1 + \left(\frac{\mu_i}{\mu_j} \right)^2 \left(\frac{W_j}{W_i} \right)^{1/4} \right]^2, \\ \lambda_{\text{eff}} &= \frac{\mu_0}{\text{Pr}} + \frac{\mu_t}{\text{Pr}_t}, \quad D_{\text{eff}} = \frac{\mu_0}{\text{Sc}} + \frac{\mu_t}{\text{Pr}_t}, \quad \text{Pr} = 0.72, \quad \text{Sc} = 0.72. \end{aligned}$$

For the constants entering into the equations, the following values recommended in [15] were used: $C_{1\varepsilon} = 1.44$, $C_{2\varepsilon} = 1.92$, $C'_{1\varepsilon} = 0.9$, $C'_{2\varepsilon} = 0.2$, $C_{3\varepsilon} = 0.8$, $\sigma_\varepsilon = 1.3$, $\sigma_k = 1$, $C_\mu = 0.09$, $\text{Pr}_t = 0.7$, and $\text{Sc}_t = 0.7$. The Sutherland coefficient γ and the values of the dynamic viscosity μ_0 at $T_* = 300$ K are given in Table 1 for various gases [16, 18]. The chemical reaction parameters were taken according to the data of [19]: $K = 2.2 \cdot 10^8$ 1/sec, $E = 104$ kJ/mole, and $B = 2$.

The system of equations (3)–(14) should be solved subject to the following boundary conditions:

$$\left. \begin{array}{l} z=0 \\ r < d/2 \end{array} \right\} \rightarrow \begin{array}{l} v_z = v_{z,\text{ent}}, \quad v_r = 0, \quad v_\varphi = \omega r, \quad k = \text{Tu} v_\varphi^2, \quad \varepsilon = \varepsilon_{\text{ent}}, \\ T = T_{\text{ent}} > T_e, \quad M_{\text{fl}} = 1, \quad M_{\text{ox}} = 0, \quad M_{\text{pr}} = 0, \quad M_{\text{in}} = 0, \end{array} \quad (15)$$

$$\left. \begin{array}{l} z=0 \\ r > d/2 \end{array} \right\} \rightarrow \begin{array}{l} v_z = 0, \quad v_r = 0, \quad v_\varphi = 0, \quad T = T_e, \\ \frac{\partial M_{\text{fl}}}{\partial z} = 0, \quad \frac{\partial M_{\text{ox}}}{\partial z} = 0, \quad \frac{\partial M_{\text{pr}}}{\partial z} = 0, \quad \frac{\partial M_{\text{in}}}{\partial z} = 0. \end{array} \quad (16)$$

To describe the turbulence parameters in the vicinity of the solid wall (underlying surface), the technique of [13] was used, according to which the values of k and ε in the first boundary node can be determined as

$$k_{n,w} = \frac{\tau_w}{\rho \sqrt{C_\mu}}, \quad \varepsilon_{n,w} = \frac{1}{\kappa z} \left(\frac{\tau_w}{\rho} \right)^{3/2}, \quad \kappa = 0.4.$$

The stress on the wall can be found as follows:

$$\tau_w = \begin{cases} \mu v_z / \delta, & Y^+ \leq 11.5; \\ A \kappa^{-1} Y^+ C_\mu^{1/4} \rho v_z \sqrt{k} \ln Y^+, & Y^+ > 11.5, \end{cases}$$

where $Y^+ = \frac{4\sqrt{C_\mu} \rho \sqrt{k} \delta R}{\mu}$; $A = 9.0$ (for a smooth wall). On the remaining boundaries the following conditions are satisfied:

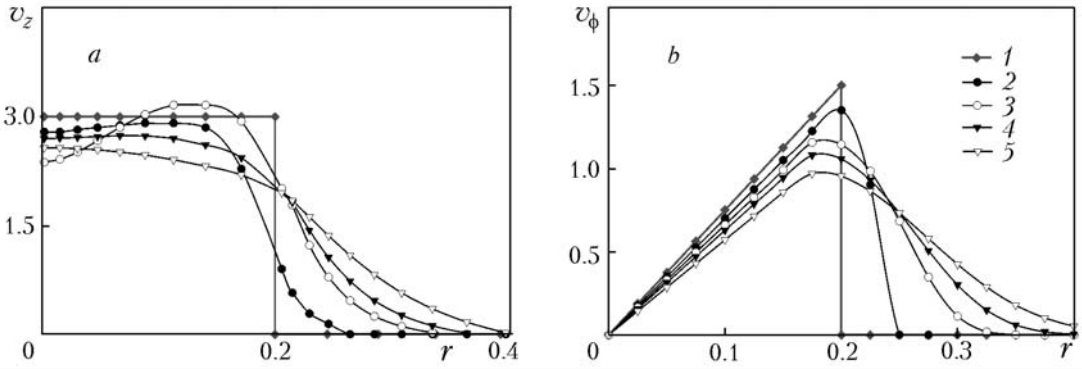


Fig. 1. Radial distribution of axial (a) and tangential (b) velocity ($\text{Ro} = 0.5$):
1) $x = 0$; 2) 0.2; 3) 0.4; 4) 0.6; 5) 1.4 m. v , m/sec; r , m.

$$r=0: \frac{\partial v_z}{\partial r}=0, \quad v_r=0, \quad v_\phi=0, \quad \frac{\partial T}{\partial r}=0, \quad \frac{\partial k}{\partial r}=0, \quad \frac{\partial \varepsilon}{\partial r}=0, \quad \frac{\partial M_{\text{fl}}}{\partial r}=0,$$

$$\frac{\partial M_{\text{ox}}}{\partial r}=0, \quad \frac{\partial M_{\text{pr}}}{\partial r}=0, \quad \frac{\partial M_{\text{in}}}{\partial r}=0; \quad (17)$$

$$r \rightarrow \infty: \quad v_z=0, \quad v_r=0, \quad v_\phi=0, \quad k=0, \quad \varepsilon=0, \quad T=T_e, \quad M_{\text{fl}}=0,$$

$$M_{\text{ox}}=M_{\text{ox}}^e, \quad M_{\text{pr}}=M_{\text{pr}}^e, \quad M_{\text{in}}=M_{\text{in}}^e; \quad (18)$$

$$z \rightarrow \infty: \quad v_z=0, \quad v_r=0, \quad v_\phi=0, \quad k=0, \quad \varepsilon=0, \quad T=T_e, \quad M_{\text{fl}}=0,$$

$$M_{\text{ox}}=M_{\text{ox}}^e, \quad M_{\text{pr}}=M_{\text{pr}}^e, \quad M_{\text{in}}=M_{\text{in}}^e. \quad (19)$$

The equations considered above were solved numerically using the finite volume method [20], a staggered grid with 210 nodes in the axial direction and 176 nodes in the radial one. In approximation of convective terms the upstream scheme of the third order of accuracy QUICK suggested by Leonard [21] was applied, the diffusion terms were approximated by the central difference scheme. The continuity equation was satisfied with the aid of the SIMPLEC algorithm [22]. It was considered that the convergence of iterations was attained if the mean-square discrepancy for all the variables did not exceed 1%.

Analysis of Results. The initial diameter of the jet d varied within the range 0.1–0.4 m, and the velocity of gas escaping into the stagnant medium and the turbulence intensity were assumed equal to $v_{z,\text{ent}} = 3$ m/sec and $T_u = 0.03$. The jet temperature at the entrance and the temperature of the environment were assumed equal to $T_{\text{ent}} = 900$ K and $T_e = 300$ K.

The twisting of a gas flow leads to the appearance of the tangential velocity component v_ϕ and to the formation of the field of centrifugal forces proportional to $\rho v_\phi^2/r$, which intensify gas motion in the radial direction. The influence of twisting on the flow structure will be characterized with the aid of the Rossby number $\text{Ro} = \frac{\omega d}{2v_{z,\text{ent}}}$.

Weak twisting ($\text{Ro} < 0.3$) practically does not change the flow picture. However, with increase in twisting in the central axial region, zones with rarefaction or smaller static pressure appear because of the centrifugal effect. Due to this, in the axial zone of flow, in the case of moderate flow twisting ($0.3 < \text{Ro} < 0.6$), troughs in the transverse profile of the axial components of the velocity vector are formed, and in the case of strong twisting ($0.6 < \text{Ro}$) reverse currents appear.

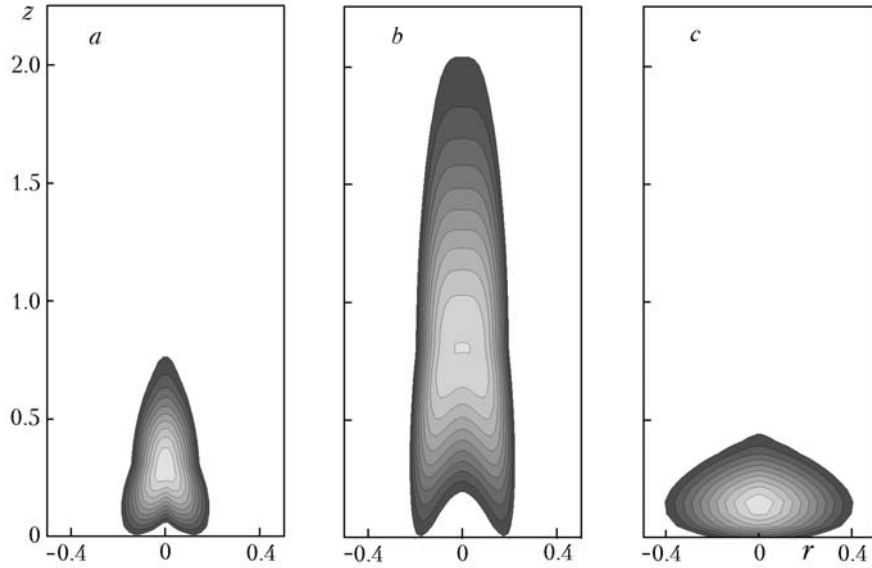


Fig. 2. Distribution of isotherms in a flow with combustion (a minimum isotherm corresponds to a temperature of 1200 K, the step between isolines is 100 K): a) $\text{Ro} = 0$; b) 0.5; c) 0.8. z, r, m .

Near the surface $z = 0$, the distribution of the axial velocity component is monotonic in the case of small twistings. Then, at $0.3 < \text{Ro} < 0.6$ the $v_z(r)$ curve acquires a characteristic form with a maximum displaced relative to the center and with a trough at the center (Fig. 1a). With distance from the entrance, the jet expands in width, then the internal zone with the velocity trough disappears, and the profile is deformed and becomes monotonic.

The flow formed contains a central core with quasisolid rotation and the external region with quasipotential rotation (Fig. 1b). Thus, the rotation can be described with the aid of a free-forced vortex, which in application to atmospheric phenomena corresponds to the formation of whirlwinds, dusty storms, and other tornado-like vortices.

The flow twisting exerts its influence not only on the flow structure, but also on the turbulence characteristics. First, it causes considerable flow velocity gradients and thereby generates turbulent stresses. Second, depending on the character of the radial distribution of velocity components, the energy may transform into a potential one and vice versa [23]. With the active character of action, the centrifugal force leads to the enhancement of turbulent pulsations, but in the case of its conservative action, to their suppression.

This is most evident in flows with moderate twisting, and not noticeable in the case of weak twisting. In strongly twisted flows the first mechanism of the influence of twisting on turbulence begins to play the major role; it is connected with the appearance of considerable gradients of averaged flow velocity and, as a consequence, with an increase in turbulent stresses.

As a result of injection of carbon monoxide, a nonisothermal turbulent jet is formed. Its propagation is characterized not only by an increase in the mixing layer thickness, but also by the formation of a nonuniform axial velocity profile. Thus, there is a region in which the gas velocity does not exceed the normal velocity of flame propagation. Usually this region is called an igniting ring and plays an important role in flame stabilization [24]. From the igniting ring the combustion propagates downstream. In this case, due to turbulent heat conduction the heat is transferred from the ignited peripheral layers into the inner layers causing their ignition, and simultaneously it is carried away downstream forming, in the absence of twisting, a cone-like torch (Fig. 2a).

With the appearance of twisting, the structure of the flame changes. In the case of initially weak twisting of the flow ($\text{Ro} < 0.3$), the flame front maintains a cone-like form due to the relative homogeneity of the axial velocity profile.

In flows with moderate intensity of twisting ($0.3 < \text{Ro} < 0.6$) relaminarization is observed; it prevents the mixing of the fuel, contained in the twisted jet, with oxygen from the air that surrounds the jet. Moreover, flow twisting leads to a considerable change in the axial velocity component profile that in the flow core becomes comparable

with the flame propagation velocity U (the so-called "retaining zone" is being formed), while on the periphery it is much higher. As a result, the distortion of the flame front occurs, whose surface acquires a column-like shape, allowing one to define such a regime of combustion as a fiery whirlwind (Fig. 2b).

If there is a strong twisting of the flow, when the combustion regime is determined by the igniting effect of combustible products in the recirculation zone, a very short torch with a very high intensity of combustion is formed (Fig. 2c). Note that the results obtained are in qualitatively agreement with the experimental data of [4, 5].

Conclusions. The formation of a fiery whirlwind can be explained by the appearance of local equilibrium in a free-forced vortex and by the anisotropy of turbulence and laminarization of a flow in the case of moderate flow twisting leading to the weakening of turbulent mixing of a combustible and an oxidant and to the lengthening of the zone of combustion.

This work was carried out with financial support from the Russian Foundation for Basic Research, grant No. 08-01-00496, as well as from the Alexander von Humboldt Foundation (Germany).

NOTATION

A , dimensionless constant in the "wall law"; B , parameter in combustion model; C , constants in the model of turbulence; c_p , specific heat at constant pressure, $J/(kg\cdot K)$; D , diffusion coefficient, m^2/sec ; d , diameter of a jet, m ; Da , Damköhler number; E , activation energy, $J/mole$; f , function in the model of turbulence; G_k , dissipation function, Pa/sec ; g , free fall acceleration, m/sec^2 ; I , function in the model of turbulence, Pa/sec ; J , function in the model of turbulence, Pa/sec ; K , preexponential factor, $m^3/(kg\cdot sec)$; k , turbulent kinetic energy, m^2/sec^2 ; M , mass concentration; P , function in the model of turbulence, Pa/sec ; p , pressure, Pa ; Pr , Prandtl number; Q , thermal effect of chemical reaction, J/kg ; R , universal gas constant, $J/(mole\cdot K)$; r , radial coordinate, m ; Re , Reynolds number; Ro , Rossby number; Sc , Schmidt number; T , temperature, K ; Tu , turbulence parameter; U , velocity of flame propagation, m/sec ; v , velocity, m/sec ; W , molecular mass, $kg/mole$; Y^+ , dimensionless distance from the wall; z , axial coordinate, m ; α , tensor of turbulence anisotropy; γ , the Sutherland coefficient, K ; δ , distance from the wall to the nearest node, m ; ε , rate of turbulent energy dissipation, m^2/sec^3 ; κ , the von Karman constant; λ , thermal conductivity, $W/(m\cdot K)$; μ , dynamic viscosity, $Pa\cdot sec$; ξ_k , molar concentration of a component; ρ , density, kg/m^3 ; σ , turbulent Prandtl number, τ_w , stresses on a wall, Pa ; Φ , chemical reaction rate, $kg/(m^3\cdot sec)$; ψ_{kj} , parameter of collisions; ω , angular velocity, rad/sec . Subscripts and superscripts: 0 , molecular; e , environment; eff , effective; ent , parameter at entrance; fl , combustible (carbon monoxide); in , inert diluent (atmospheric air nitrogen); $n.w$, near-wall node; ox , oxidant (oxygen); pr , reaction product (carbon dioxide); t , turbulent; w , wall; μ , viscosity; $*$, characteristic value.

REFERENCES

1. A. M. Grishin, *Mathematical Simulation of Forest Fires and Novel Means of Combating Them* [in Russian], Nauka, Novosibirsk (1992).
2. Yu. A. Gostintsev and S. S. Novikov, On the vortical structure of a rapidly propagating fire, *Fiz. Goreniya Vzryva*, No. 3, 403–412 (1975).
3. Yu. A. Gostintsev, G. M. Makhviladze, and B. V. Novozhilov, Formation of a large fire caused by radiation, *Izv. Ross. Akad. Nauk, Mekh. Zhidk. Gaza*, No. 1, 17–25 (1992).
4. A. M. Grishin, A. N. Golovanov, and Ya. V. Sukov, Physical modeling of fire tornadoes, *Dokl. Ross. Akad. Nauk*, **395**, No. 2, 196–198 (2002).
5. A. M. Grishin, A. N. Golovanov, A. A. Kolesnikov, A. A. Strokatov, and R. Sh. Tsvykh, Experimental investigation of thermal and fire tornadoes, *Dokl. Ross. Akad. Nauk*, **400**, No. 5, 618–620 (2005).
6. 8. B. Gebhart, Y. Jaluria, R. L. Mahajan, and B. Sammaki, *Buoyancy-Induced Flows and Transport* [Russian translation], Vol. 1, Mir, Moscow (1991).
7. S. V. Alekseenko, P. A. Kuibin, and V. L. Okulov, *Introduction to the Theory of Concentrated Vortices* [in Russian], ITF SO RAN, Novosibirsk (2003).
8. A. K. Gupta, D. G. Lilley, and N. Syred, *Swirl Flows* [Russian translation], Mir, Moscow (1987).

9. A. Yu. Snegirev., J. A. Marsden, J. Francis, and G. M. Makhviladze, Numerical studies and experimental observations of whirling flames, *Int. J. Heat Mass Transfer*, **47**, 2523–2539 (2004).
10. A. M. Grishin and O. V. Matvienko, Mathematical simulation of fire tornadoes, in: *Abstracts of Papers and Communications at the 5th Minsk Int. Heat and Mass Transfer Forum* [in Russian], Vol. 1, ITMO NAN Belarusi, Minsk (2004), pp. 174–176.
11. A. M. Grishin, O. V. Matvienko, and Yu. A. Rudi, Mathematical simulation of the formation of thermal tornadoes, in: *Abstracts of Papers and Communications at the 6th Minsk Int. Heat and Mass Transfer Forum* [in Russian], Vol. 1, ITMO NAN Belarusi, Minsk (2008), pp. 204–206.
12. D. Lilly, Combustion in swirling flows. A review, *Raketn. Tekhn. Kosmonavt.*, No. 8, 12–19 (1977).
13. M. A. Leschziner and W. Rodi, Computation of strongly swirling axisymmetric free jets, *AIAA J.*, **22**, No. 11, 370–373 (1984).
14. T. Kobayashi and M. Yoda, Modified $k-\epsilon$ -model for turbulent swirling flow in a straight pipe, *JSME Int. J.*, **30**, 66–71 (1987).
15. J. Piquet, *Turbulent Flows: Models and Physics*, Springer, Berlin (1999).
16. O. G. Martynenko (Ed.), *Handbook on Heat Exchangers* [in Russian], Vol. 1, Energoatomizdat, Moscow (1987).
17. V. V. Pomerantsev (Ed.), *Principles of the Practical Theory of Combustion* [in Russian], Energoatomizdat, Moscow (1986).
18. J. Warnatz, U. Maas, and R. W. Dibble, *Combustion*, Springer (1999).
19. C. K. Westbrook and F. L. Dryer, Chemical kinetic modeling of hydrocarbon combustion, *Prog. Energy Combust. Sci.*, **10**, 1–57 (1984).
20. S. Patankar, *Numerical Methods for Solving Problems of Heat Transfer and Fluid Dynamics* [Russian translation], Energoatomizdat, Moscow (1983).
21. B. P. Leonard, A stable and accurate convection modelling procedure based on quadratic upstream interpolation, *Comput. Meth. Appl. Mech. Eng.*, **19**, 59–98 (1979).
22. J. P. Van Doormal and G. D. Raithby, Enhancements of the SIMPLE method for predicting incompressible fluid flow, *Numer. Heat Transfer*, **7**, 147–163 (1984).
23. A. A. Khalatov, *Theory and Practice of Twisted Flows* [in Russian], Naukova Dumka, Kiev (1989).
24. D. M. Khzmalyan, *Theory of Furnace Processes* [in Russian], Energoatomizdat, Moscow (1990).